AAC Journals.ASM.org

An Altered *Mycobacterium tuberculosis* Metabolome Induced by *katG* Mutations Resulting in Isoniazid Resistance

Du Toit Loots*

Centre for Human Metabonomics, School for Physical and Chemical Sciences, North-West University, Potchefstroom, South Africa

The most common form of drug resistance found in tuberculosis (TB)-positive clinical samples is monoresistance to isoniazid. Various genomics and proteomics studies to date have investigated this phenomenon; however, the exact mechanisms relating to how this occurs, as well as the implications of this on the TB-causing organisms function and structure, are only partly understood. Considering this, we followed a metabolomics research approach to identify potential new metabolic pathways and metabolite markers, which when interpreted in context would give a holistic explanation for many of the phenotypic characteristics associated with a *katG* mutation and the resulting isoniazid resistance in *Mycobacterium tuberculosis*. In order to achieve these objectives, gas chromatography-time of flight mass spectrometry (GCxGC-TOFMS)-generated metabolite profiles from two isoniazid-resistant strains were compared to a wild-type parent strain. Principal component analyses showed clear differentiation between the groups, and the metabolites best describing the separation between these groups were identified. It is clear from the data that due to a mutation in the *katG* gene encoding catalase, the isoniazid-resistant strains experience increased susceptibility to oxidative stress and have consequently adapted to this by upregulating the synthesis of a number of compounds involved in (i) increased uptake and use of alkanes and fatty acids as a source of carbon and energy and (ii) the synthesis of a number of compounds directly involved in reducing oxidative stress, including an ascorbic acid degradation pathway, which to date hasn't been proposed to exist in these organisms.

The discovery of isoniazid/isonicotinic acid hydrazide in 1945 was considered a major breakthrough in the treatment of tuberculosis (TB), as this drug exhibited high antimicrobial activity with relatively few side effects, in addition to it being relatively inexpensive (1). Isoniazid requires *in vivo* activation before it exhibits any of its antimicrobial effects (2, 3). This activation occurs via the bacterial enzyme catalase-peroxidase to form isonicotinoyl radicals, which in turn reacts with NAD, and the resulting conjugates bind to the NAD(H) recognition site of the enzyme InhA (4), inhibiting its action. InhA is an enoyl-acyl carrier protein, primarily involved in bacterial fatty acid elongation via the FAS II system and essential for mycolic acid synthesis (5, 6). Consequently, inhibition of InhA by isoniazid results in disruption of normal cell wall structure and functioning and the death of the TB-causing bacteria.

However, within a few months of isoniazid's introduction as an anti-TB drug, frequent reports of rapid resistance to this started emerging (7). Consequently, various combination treatment approaches were introduced and are still being used to this day. Monoresistance to isoniazid is the most common form of drug resistance found in clinical samples, constituting approximately 13.3% of all reported global TB cases (8). The majority of these isoniazid-resistant strains (40 to 58%) are attributed to a mutation in the primary mycobacterial catalase-peroxidase gene (*katG*), which possesses both catalase and peroxidase activities (9). This mutation results in an enzyme that is unable to activate isoniazid but retains 50% of its catalase-peroxidase function. Consequently, these mutants are resistant to isoniazid but retain a sufficient level of oxidative protection to maintain the organism's resistance to the host's induced antibacterial oxidation mechanisms (10).

The most frequent *katG* mutation detected in clinical samples is Ser-315, deleted or altered to either threonine, asparagine, isoleucine, arginine, or glycine (11). A mutation in this region results in a decreased affinity of the enzyme to bind isoniazid. Other less frequent mutations detected in *katG* result in various levels of isoniazid resistance and catalase-peroxidase activities (12) and include mutations in the D36E, H108Q, T262R, A350S, and G629S functional residues of the enzyme (13). Furthermore, mutations in the promoter region of the alkyl hydroperoxidase reductase (*ahpC*) gene of *Mycobacterium tuberculosis* [G(−48)A, G(−51)A, C(−54)T, G(−74)A, and C(−81)T)] have also been associated with isoniazid resistance (13). These were, however, also accompanied by mutations in *katG* and resulted in a complete loss of the enzyme's catalase-peroxidase functioning (12). Consequently, these *ahpC* mutations, detected in 10% of all isoniazid-resistant strains, are not directly implicated in isoniazid drug resistance, and the resultant overexpression of alkyl hydroperoxidase reductase is thought to be a method by which these organisms compensate for their loss of catalase-peroxidase activity (14).

As described above, the majority of the research explaining isoniazid drug resistance was done using genomic techniques, involving gene chips (15) and genomic sequencing (8), subsequently identifying the underlying mutations responsible for the observed phenotypical changes. From a proteomics perspective, the three-dimensional (3D) crystal structures of the enzymes involved in drug resistance have also been studied, for the purpose of identifying the specific drug binding sites and possible enzyme structure alterations, which occur due to the these mutations (16).

Received 29 October 2013 **Returned for modification** 18 November 2013
Accepted 19 January 2014
Published ahead of print 27 January 2014
Address correspondence to Du Toit Loots, Dutoit.Loots@nwu.ac.za.
* Present address: Centre for Human Metabolomics, Potchefstroom, South Africa.

doi:10.1128/AAC.02344-13

Furthermore, the interactome of *M. tuberculosis* was studied (17), investigating those pathways potentially causing drug resistance. However, no study examining this phenomenon from a metabolomics perspective has been attempted, until now. Metabolomics is a relatively new research direction, aimed at investigating various cell/disease mechanisms from a metabolic profile perspective. Metabolomics can be defined as "the nonbiased identification and quantification of all the metabolites in a biological system," using highly sensitive analytical procedures (18). This approach serves as the basis for the discovery of new biomarkers for better disease diagnosis and for better describing the mechanisms resulting in drug resistance, elucidating drug mechanisms, and monitoring treatment outcomes (3).

Considering this, we applied a metabolomics research approach, using two-dimensional gas chromatography-time of flight mass spectrometry (GCxGC-TOFMS), and compared the metabolomes of two different isoniazid-resistant strains of *M. tuberculosis* (H15 and H71) to that of a wild-type TB72 parent strain. The metabolite markers identified were subsequently interpreted in the light of the *katG* mutations, and by using the proposed approach (19), we were able to generate a more holistic understanding of the underlying mechanisms relating to mutations in *katG* and the resulting drug resistance to isoniazid in *M. tuberculosis*.

MATERIALS AND METHODS

Bacterial cultures and selection of isoniazid resistance strains. The two isoniazid drug-resistant *M. tuberculosis* strains (H15, $n = 8$ cultures; H71, $n = 8$ cultures) and the wild-type *M. tuberculosis* parent strain (ATCC 35801) ($n = 8$ cultures), belonging to the Haarlem genotype, were cultured and selected by the Royal Tropical Institute, Amsterdam, The Netherlands, as previously described (8). The reason for using the above-given approach is to generate mutants with a resistance mechanism/mutation more closely resembling that seen by *in vivo* isolated isoniazid mutant strains. The DNA isolation of the isoniazid-resistant strains and characterization of the isoniazid resistance-conferring *katG* mutations was done via PCR and sequencing of a 233-bp fragment surrounding codon 315 and a 300-bp fragment surrounding codon 463 of *katG*, as previously described (8). The mutation causing isoniazid resistance in the H15 strain was due to a mutation at codon 321 of the *katG* gene, resulting in phenylalanine replacing tryptophan in the amino acid sequence of the translated catalase-peroxidase enzyme. The H71strain, on the other hand, is characterized by a deletion of codon 315 of the *katG* gene (20).

Both the isoniazid-resistant and wild-type parent strains were then cultured in Middlebrook 7H9 broth supplemented with oleic acid-albumin-dextrose in a shaking incubator at 37°C. For each strain, liquid starting cultures were made by inoculating pure colonies into 10 ml culture medium until these cultures reached the logarithmic growth phase. Prior to extraction, the bacteria were isolated from each culture ($n = 8$) for each of the three strains, snap-frozen, lyophilized, and stored at −80°C until sample extraction.

Sample extraction. Five milligrams of each lyophilized sample was weighed into a prewashed (with 0.5 ml chloroform, 0.5 ml methanol, and 0.5 ml Nanopure water, followed by shaking in a vibration mill for 3 min with a carbide tungsten bead at 30 Hz · s^{-1}) 1.5-ml microcentrifuge tube, followed by the addition of 50 μl 3-phenylbutyric acid (0.104 μg/ml), as the internal standard. A mixture of chloroform, methanol, and water (1 ml) was added in the ratio of 1:3:1, briefly vortexed, and then placed in a vibration mill (Retsch, Haan, Germany) with a carbide tungsten bead (Retsch) for 5 min at 30 Hz · s^{-1}. The sample was then centrifuged for 7 min at 12,000 rpm at 4°C, and the supernatant was subsequently transferred to a 2-ml glass sample vial (Separations, Johannesburg, South Africa) and dried under a stream of nitrogen at room temperature.

Samples were then derivatized using 50 μl methoxyamine hydrochloride (containing 15 mg/ml pyridine) at 50°C for 90 min, followed by 50 μl *N*-methyl-*N*-(trimethylsilyl)trifluoroacetamide with 1% trimethylchlorosilane at 50°C for 60 min. The samples were subsequently transferred to a 0.1-ml insert in a 2-ml sample vial and capped prior to GCxGC-TOFMS analysis.

GCxGC-TOFMS analysis. Analyses of the derivatized samples were done using a Pegasus 4D (LECO Corporation, St. Joseph, MI, USA) two-dimensional time of flight mass spectrometer (GCxGC-TOFMS), equipped with an Agilent 7890A gas chromatograph (Agilent, Atlanta, GA), a secondary oven, a dual-stage cryomodulator, and a Gerstel multipurpose sampler 2-XL (MPS2-XL) (Gerstel GmbH & Co. KG, Mülheim an der Ruhr, Germany). The primary column used was a Restek Rxi-5Sil MS capillary column (30 m, 0.25 mm internal diameter [i.d.], 0.25 μm phase film thickness [d.f.]) and a Restek Rxi-17 (1 m, 100 μm i.d., 0.1 μm d.f.) served for secondary column separation. The derivatized samples (1 μl) were injected at a 5:1 split ratio, and helium was used as the carrier gas at a constant flow rate of 1 ml/min. The injector temperature was held constant at 270°C for the entire run. An initial oven temperature for the primary column was 70°C and was maintained for 2 min, followed by an increase of 4°C/min, until a final temperature of 300°C was reach and maintained for an additional 2 min. Cryomodulation and a hot pulse of compressed air for 0.7 s, every 3 s, was used to control the effluent off the primary column and onto the secondary column. The secondary column oven temperature program was identical to that of the primary column, with a +5°C offset. No mass spectra were recorded for the first 550 s of each run (solvent delay). The transfer line temperature was held at a constant 280°C and the ion source at a constant 200°C for the entire run. The detector voltage was 1,700 V, and the filament bias was −70 eV. Mass spectra were collected from 50 to 800 *m*/*z* at an acquisition rate of 100 spectra per second.

Deconvolution and peak alignment. LECO Corporation ChromaTOF software (version 4.32) was used for peak identification and mass spectral deconvolution (signal-to-noise ratio of 200). Compound identification was done by comparison of the mass spectra and relative retention indices of the detected compounds to a library compiled from previously injected standards. To eliminate the effect of retention time shifts, peaks with similar mass spectra were aligned across all samples using an optional peak alignment function of the ChromaTOF software Statistical Compare. Peak areas were normalized relative to the internal standards by calculating the relative concentration of each compound.

Statistical data analysis. Compounds which were detected in less than 50% of the samples in any sample group or showed no variation between the groups were removed. A quality control (QC) correction step was applied to the data set using quantile equating to correct for linear and nonlinear differences in distribution (21). Zero value replacement substituted the zero value of undetected compounds with a value calculated as half of the minimum concentration in the original data to account for the detection limit of the apparatus, and a QC-coefficient of variation (CV) filter of 50% was applied (22).

Statistical data analysis was done using MetaboAnalyst, a metabolomics Web server based on statistical package "R" version 2.10.0 and supported by The Metabolomics Innovation Centre (TMIC). The data set was log transformed. Principle component analysis (PCA) was performed to determine whether a natural differentiation exists between the sample groups based on their metabolite profiles. PCA transforms a number of possibly related variables (or metabolites) into a smaller number of unrelated variables known as principal components (PCs), which express the maximum variation in the data set by characterizing each component in a multidimensional space. The PCA modeling power of each metabolite was determined, and those with a modeling power of greater than 0.5 were considered important in determining the differentiation of the groups (23).

Univariate analysis, including effect size (ES), as described previously (24), was used to evaluate the importance of the variation of individual

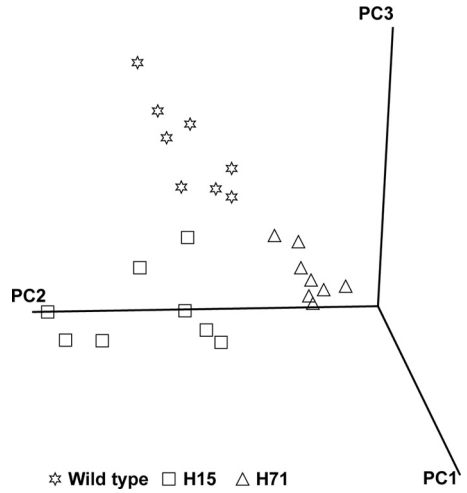

FIG 1 A three-dimensional PCA score plot indicating the natural grouping and differentiation of the individual samples into the respective isoniazid-resistant strain groups H15 and H71 and the wild-type MTB72 parent strain, due to variation in their metabolic profiles (PC1, 87%; PC2, 2.7%; and PC3, 2.1%).

metabolites. For this nonparametric data set, an effect size of >0.5 is considered to be highly relevant, >0.3 potentially relevant, and <0.1 irrelevant. Descriptive statistics based on the unscaled data includes means and standard deviations.

RESULTS

A total of 736 compound peaks were identified after GCxGC-TOFMS analyses in each of the samples extracted. Multivariate statistics was used to determine if a natural differentiation exists between the groups on the basis of these detected compounds using PCA. As can be seen in Fig. 1, PCA of the GCxGC-TOFMS metabolome data shows clear differentiation between the two isoniazid-resistant *M. tuberculosis* strains and the wild-type parent strain. This can be ascribed to the metabolite profiles of these 3 groups varying significantly enough to allow for a natural grouping of the individual samples into their respective groups. Subsequently, those compounds that contribute most to the variation determined between the analyzed sample groups were identified and used as potential markers for explaining the variation between the isoniazid-resistant strains (H15 and H71) and the wild-type parent strain, for the purpose of elucidating the mechanisms relating to isoniazid resistance from a metabolomics perspective (Table 1). Of these 29 compounds identified, 23 could be annotated using the libraries and 6 remained unknown. These metab-

TABLE 1 The mean concentrations and standard deviations of compounds contributing the most to the variation between the isoniazid-resistant *M. tuberculosis* and wild-type MTB72 parent strain, as determined by the PCA projections

Compound	Concn (SD) (μg/mg of sample)			PCA power	Effect size
	Wild type	H15	H71		
Alkanes					
Decane	0.24 (0.30)	2.07 (0.85)	1.47 (0.41)	0.684	1.64
Hexadecane	0	2.13 (1.25)	1.32 (0.28)	0.637	1.30
Dodecane	0.29 (0.17)	1.89 (0.43)	1.18 (0.32)	0.586	1.65
Heptadecane	0 (0)	1.50 (0.62)	0.50 (0.40)	0.580	1.34
Tridecane	0.47 (0.25)	1.98 (0.52)	0.78 (0.37)	0.501	1.01
2-Methyl-tridecane	0.27 (0.121)	3.03 (1.08)	0.78 (0.37)	0.500	1.01
Alcohols					
Tridecanol	1.77 (0.56)	7.98 (3.59)	5.74 (2.24)	0.764	0.73
Isotridecanol	0.49 (0.59)	2.58 (0.30)	2.19 (0.88)	0.755	1.70
Dodecanol	0	0.90 (0.80)	0.16 (0.08)	0.695	1.55
Decanol	0.02 (0.02)	0.21 (0.01)	0.17 (0.06)	0.523	1.22
Fatty acids					
Eicosonoic acid	0.29 (0.07)	0.45 (0.14)	0.93 (0.24)	0.825	0.92
Hexadecanoic acid	0.82 (0.19)	2.81 (0.87)	2.72 (0.38)	0.755	1.20
Nonadecanoic acid	2.46 (0.45)	2.86 (0.35)	4.24 (0.48)	0.746	0.81
Octadecanoic acid	4.37 (0.94)	8.95 (2.36)	10.37 (3.47)	0.737	1.08
2-Methyl-hexadecanoic acid	0.46 (0.14)	0.42 (0.12)	0.16 (0.09)	0.727	1.20
Heptadecanoic acid	0.27 (0.06)	0.51 (0.10)	0.95 (0.16)	0.686	3.39
Decanoic acid	0.03 (0.01)	0.04 (0.02)	0.04 (0.004)	0.685	0.55
Dodecanoic acid	0.02 (0.01)	0.03 (0.02)	0.03 (0.01)	0.521	1.22
Compounds related to a direct adaption to oxidative stress					
Threonic acid	0.02 (0.01)	0.03 (0.006)	0.04 (0.002)	0.690	0.72
Cadaverine	0.17 (0.04)	0.64 (0.07)	0.59 (0.07)	0.650	1.67
p-Hydroxybenzoic acid	0.02 (0.01)	0.21 (0.02)	0.18 (0.05)	0.546	0.64
Other					
D-Glycero-L-manno-heptonic acid	0	0.04 (0.02)	0.03 (0.01)	0.802	2.97
n-Butylamine	0.1 (0.05)	0.07 (0.06)	0.03 (0.007)	0.771	2.81

olite markers were classified into their respective compound groups and included mostly corresponding alkanes, alcohols, and fatty acids, a surfactant known to assist in the uptake and utilization of these compounds as alternative energy sources, and various compounds known to be associated with oxidative stress. The majority of these compounds were additionally detected in elevated concentrations in the isoniazid-resistant strains comparatively.

DISCUSSION

Aerobic organisms, including *M. tuberculosis*, require oxygen for respiration and the oxidation of nutrients for energy production. However, damaging reactive by-products, such as superoxide anion radicals, hydrogen peroxide, and reactive hydroxyl radicals, are usually generated during these processes (25). Additionally, the host also responds to *M. tuberculosis* infection by generating an oxidative stress onslaught, once engulfed by host macrophages as part of the host immune response (11). In order for these bacteria to survive these oxidative conditions, they possess a series of defense mechanisms, including (i) detoxifying enzymes and scavengers for free radicals, (ii) various DNA and protein repair systems, and (iii) increased usage of nutrient substrates ensuring bacterial survival (10). The *katG* gene encodes the catalase-peroxidase enzyme, which traditionally serves to protect these organisms from oxidative stress. Apart from this, the *oxyR* gene, considered to be the primary regulator of the peroxide stress responses in Gram-negative bacteria, activated by exposure to low dosages of hydrogen peroxide, expresses at least 9 proteins able to protect the cell against these oxidative stress conditions (26). The *oxyR* gene is additionally responsible for the hydrogen peroxide-dependent induction of *katG* expression (27). Wild-type *M. tuberculosis*, however, seems to have a reduced defense against reactive oxygen species (28) comparative to other aerobic organisms, due to a series of mutations detected in its *oxyR* gene region, resulting in a total loss of *oxyR* functionality (29). Gupta and Chatterji, however, speculate that due to the fact that the oxidative stress response is crucial to the survival of this organism, this pathway has become constitutive rather than inducible, hence no longer requiring a positive regulator (30). *M. tuberculosis* has potentially developed other mechanisms for regulating the expression of *katG*. One of these is thought to be the *ahpC* gene, which codes for a subunit of an organic peroxide detoxification enzyme found in these bacteria. However, the expression of *ahpC* in *M. tuberculosis* was found to be rather low, and its expression was found not to be upregulated during periods of oxidative stress (31). Jaeger et al. determined that isolates unable to overexpress AhpC were in fact avirulent, and they consequently concluded that AhpC is an important virulence factor, especially in isoniazid-resistant strains (32). More recently, *oxyS* has been shown to directly regulate *katG* in response to oxidative stress, by binding to its promoter region, and the conserved binding site for OxyS in the promoter region of *katG* has been mapped (33).

Considering the metabolomics data collected and the markers described in Table 1, it is evident that the isoniazid-resistant strains show elevated concentrations of various alkanes, corresponding fatty acids, and alcohols. Alkanes are used by most bacteria as a carbon source, and their uptake is dependent on the type of bacteria, the length of the alkane, its availability, and the environment in which these bacteria grow (34). These alkane-utilizing bacteria secrete glycolipid surfactants, which allow for the cellular uptake and usage of these alkanes (35). Degradation of alkanes with two or more carbons starts with the oxidation of the terminal methyl group by alkane hydroxylases, yielding the corresponding primary alcohol, which in turn is oxidized by alcohol dehydrogenase to an aldehyde and then eventually converted to a fatty acid (34) to be used as an energy source or for cell wall synthesis. Schnappinger et al. recently reported that when *M. tuberculosis* resides intraphagosomally, it encounters high levels of oxidative stress, and during these conditions its dependence on the oxidation of fatty acids as a carbon source and energy source increases (36). The isoniazid-resistant strains investigated in the current study, due to the mutations in their *katG* gene, most likely experience comparatively elevated oxidative stress and consequently compensate for this by increasing the uptake of available alkanes in order to synthesize more fatty acids for utilization as a carbon and energy source (10) during such conditions. Further evidence supporting this is the increased concentrations of D-glycero-L-mannoheptonic acid in the isoniazid-resistant mutants, which is a glycolipid functioning as a surfactant assisting in the uptake of alkanes or other nutrients from the growth medium (35). Additionally, mycobacteria are one of the few bacterial species able to utilize secondary amines as carbon and nitrogen source (37). Considering this, the reduction in *N*-butylamine in the isoniazid-resistant strains further substantiates the proposed increased energy, carbon, and nitrogen demands of these organisms, due to oxidative stress induced by the absence of *katG*.

The elevated levels of *p*-hydroxybenzoic acid, cadaverine, and threonic acid detected in the isoniazid-resistant strains (Table 1) further confirm the proposed increased oxidative stress and the above-mentioned adaptive metabolism detected in these strains. *p*-Hydroxybenzoic acid is a precursor for ubiquinone synthesis in Gram-negative bacteria (38), which in turn is a well-known scavenger for peroxyl radicals, subsequently used by these bacteria for preventing lipid peroxidation of fatty acids, predominantly in the bacterial cell envelope (39). Similarly, cadaverine, an antioxidant polyamine, is also used by bacteria to prevent oxidative damage by free radicals. This compound functions either by directly neutralizing hydrogen peroxide and/or as a free radical scavenger (40). Tkachenko et al. additionally determined that various polyamines, including cadaverine, are capable of upregulating *katG* expression under conditions of oxidative stress (41). Considering this, the increased concentrations of *p*-hydroxybenzoic acid and cadaverine in the isoniazid-resistant strains are most likely due to an upregulation in their synthesis in an attempt to compensate for their reduced catalase and catalase-peroxidase activities. Furthermore, ascorbic acid is a well-known antioxidant, and elevated ascorbic acid oxidation to threonic acid, in various other organisms is usually indicative of increased oxidative stress (42). Although an ascorbic acid synthesis pathway has been previously described for *M. tuberculosis* (43), the oxidative breakdown product of this, threonic acid, most probably induced by elevated hydrogen peroxide, as detected in these isoniazid-resistant strains, has never been described for *M. tuberculosis*. This may be due to two possible reasons: first, the elevated hydrogen peroxide due to the mutation in *katG*, and second, the elevated ascorbic acid synthesis by the organism to cope with this, or both.

In conclusion, although a mutation in the *katG* gene allows *M. tuberculosis* to survive treatment with isoniazid, it would be expected to compromise its growth and viability under standard growth conditions, due to an increased susceptibility to oxidative

stress. The characteristic metabolites identified in this metabolomics approach support the notion that these organisms have upregulated a number of compensatory mechanisms for coping with this state, including (i) increased uptake and use of alkanes and fatty acids as a source for carbon and energy and (ii) the synthesis of a number of compounds directly involved in reducing oxidative stress. One should keep in mind that metabolomics investigations can be seen as the first hypothesis-generating step in the elucidation of previously unknown mechanisms, and future studies, aimed at confirming these pathways, using more direct methodology should always be considered.

ACKNOWLEDGMENTS

We thank the Royal Tropical Institute (KIT), Amsterdam, The Netherlands, for providing access to the bacterial samples and Hans de Ronde for performing bacterial cultures.

REFERENCES

1. **Zhang Y.** 2005. The magic bullets and tuberculosis drug targets. Annu. Rev. Pharmacol. **45:**529–564. http://dx.doi.org/10.1146/annurev.pharmtox.45.120403.100120.
2. **Hazbón MH, Brimacombe M, Bobadilla del Valle M, Cavatore M, Guerrero MI, Varma-Basil M, Billman-Jacobe H, Lavender C, Fyfe J, García-Garciá L, León CI, Bose M, Chaves F, Murray M, Eisenach KD, Sifuentes-Osornio J, Cave MD, Ponce de León A, Alland D.** 2006. Population genetics study of isoniazid resistance mutations and evolution of multidrug-resistant *Mycobacterium tuberculosis*. Antimicrob. Agents Chemother. **50:**2640–2649. http://dx.doi.org/10.1128/AAC.00112-06.
3. **Olivier I, Loots DT.** 2011. An overview of tuberculosis treatments and diagnostics. What role could metabolomics play? J. Cell Tissue Res. **11:**2655–2671.
4. **Janin YL.** 2007. Antituberculosis drugs: ten years of research. Bioorg. Med. Chem. **15:**2479–2513. http://dx.doi.org/10.1016/j.bmc.2007.01.030.
5. **Dessen A, Quemard A, Blanchard JS, Jacobs WR, Jr, Sachettini JC.** 1995. Crystal structure and function of the isoniazid target of *Mycobacterium tuberculosis*. Science **267:**1638–1641. http://dx.doi.org/10.1126/science.7886450.
6. **Scior T, Morales IM, Eisele SJG, Domeyer D, Laufer S.** 2002. Antitubercular isoniazid and drug resistance of *Mycobacterium tuberculosis*. Arch. Pharm. **335:**511–525. http://dx.doi.org/10.1002/ardp.200290005.
7. **Fox W, Sutherland I.** 1995. The clinical significance of positive cultures and of isoniazid-resistant tubercle bacilli during the treatment of pulmonary tuberculosis. Thorax **10:**85–98.
8. **Bergval IL, Schuitema ARJ, Klatser PR, Anthony RM.** 2009. Resistant mutants of *Mycobacterium tuberculosis* selected *in vitro* do not reflect the *in vivo* mechanism of isoniazid resistance. J. Antimicrob. Chemother. **64:**515–523. http://dx.doi.org/10.1093/jac/dkp237.
9. **Heym B, Zhang Y, Poulet S, Young D, Cole ST.** 1993. Characterization of the *katG* gene encoding a catalase-peroxidase required for the isoniazid susceptibility of *Mycobacterium tuberculosis*. J. Bacteriol. **175:**4255–4259.
10. **Hassett DJ, Cohen MS.** 1989. Bacterial adaptation to oxidative stress: implications for pathogenesis and interaction with phagocytic cells. FASEB J. **3:**2574–2582.
11. **Pym AS, Saint-Joanis B, Cole ST.** 2002. Effect of *katG* mutations on the virulence of *Mycobacterium tuberculosis* and the implication for transmission in humans. Infect. Immun. **70:**4955–4960. http://dx.doi.org/10.1128/IAI.70.9.4955-4960.2002.
12. **Somoskovi A, Parsons LM, Salfinger M.** 2001. The molecular basis of resistance to isoniazid, rifampin, and pyrazinamide in *Mycobacterium tuberculosis*. Respir. Res. **2:**164–168. http://dx.doi.org/10.1186/rr54.
13. **Slayden RA, Barry CE.** 2000. The genetics and biochemistry of isoniazid resistance in *Mycobacterium tuberculosis*. Microbes Infect. **2:**695–699. http://dx.doi.org/10.1016/S1286-4579(00)00359-2.
14. **Gillespie SH.** 2002. Evolution of drug resistance in *Mycobacterium tuberculosis*: clinical and molecular perspective. Antimicrob. Agents Chemother. **46:**267–274. http://dx.doi.org/10.1128/AAC.46.2.267-274.2002.
15. **Fu LM, Shinnick TM.** 2007. Understanding the action of INH on a highly INH-resistant *Mycobacterium tuberculosis* strain using Genechips. Tuberculosis **87:**63–70. http://dx.doi.org/10.1016/j.tube.2006.04.001.
16. **Bertrand T, Eady NAJ, Jones JN, Jesmin Nagy JM, Jamart-Grégoire B, Raven EL, Brown KA.** 2004. Crystal structure of *Mycobacterium tuberculosis* catalase-peroxidase. J. Biol. Chem. **279:**38991–38999. http://dx.doi.org/10.1074/jbc.M402382200.
17. **Raman K, Chandra N.** 2008. *Mycobacterium tuberculosis* interactome analysis unravels potential pathways to drug resistance. BMC Microbiol. **8:**234. http://dx.doi.org/10.1186/1471-2180-8-234.
18. **Dunn WB, Bailey NJC, Johnson HE.** 2005. Measuring the metabolome: current analytical technologies. Analyst **130:**606–625. http://dx.doi.org/10.1039/b418288j.
19. **Schoeman JC, Loots DT.** 2011. Improved disease characterization and diagnostics using metabolomics: a review. J. Cell Tissue Res. **11:**2673–2683.
20. **Bergval I, Kwok B, Schuitema A, Kremer K, van Soolingen D, Klatser P, Anthony R.** 2012. Preexisting isoniazid resistance, but not the genotype of *Mycobacterium tuberculosis* drives rifampicin resistance codon preference *in vitro*. PLoS One **7**(1):e29108. http://dx.doi.org/10.1371/journal.pone.0029108.
21. **Draisma HHM, Reijmers TH, Van der Kloet F, Bobeldijk-Pastotova I, Spies-Faber E, Vogels JTWE, Meulman JJ, Boomsma DI, Van der Greef J, Hankemeier T.** 2010. Equating, or correction for between-block effects with application to body fluid LC-MS and NMR metabolomics data sets. Anal. Chem. **82:**1039–1046. http://dx.doi.org/10.1021/ac902346a.
22. **Schoeman JC, Du Preez I, Loots DT.** 2012. A comparison of four sputum preextraction preparation methods for identifying and characterising *Mycobacterium tuberculosis* using GCxGC-TOFMS metabolomics. J. Microbiol. Methods **91:**301–311. http://dx.doi.org/10.1016/j.mimet.2012.09.002.
23. **Brereton RG.** 2003. Chemometrics. Data analysis for the laboratory and chemical plant. J. Chemometrics **17:**360–361.
24. **Field AP.** 2009. Discovering statistics using SPSS, 3rd ed, p 1–821. Sage Publications, London, United Kingdom.
25. **Cabiscol E, Tamarit J, Ros J.** 1999. Oxidative stress in bacteria and protein damage by reactive oxygen species. Internatl. Microbiol. **3:**3–8.
26. **Sherman DR, Sabo PJ, Hickey MJ, Arain TM, Mahairas GG, Yuan Y, Barry CE III, Stover K.** 1995. Disparate responses to oxidative stress in saprophytic and pathogenic mycobacteria. Proc. Natl. Acad. Sci. U. S. A. **92:**6625–6629. http://dx.doi.org/10.1073/pnas.92.14.6625.
27. **Farr S, Kogoma T.** 1991. Oxidative stress responses in *Escherichia coli* and *Salmonella typhimurium*. Microbiol. Rev. **55:**561–585.
28. **Springer B, Kidan YG, Prammananan T, Ellrott K, Böttger EC, Sander P.** 2001. Mechanisms of streptomycin resistance: selection of mutations in the 16S rRNA gene conferring resistance. Antimicrob. Agents Chemother. **45:**2877–2884. http://dx.doi.org/10.1128/AAC.45.10.2877-2884.2001.
29. **Deretic V, Song J, Pagán-Ramos E.** 1997. Loss of *oxyR* in *Mycobacterium tuberculosis*. Trends Microbiol. **5:**367–372. http://dx.doi.org/10.1016/S0966-842X(97)01112-8.
30. **Gupta S, Chatterji D.** 2005. Stress responses in mycobacteria. IUBMB Life **57:**149–159. http://dx.doi.org/10.1080/15216540500090611.
31. **Springer B, Master S, Sander P, Zahrt T, McFalone M, Song J, Papavinasundaram KG, Colston MJ, Boettger E, Deretic V.** 2001. Silencing of oxidative stress response in *Mycobacterium tuberculosis*: expression patterns of *ahpC* in virulent and avirulent strains and effect of *ahpC* inactivation. Infect. Immun. **69:**5967–5973. http://dx.doi.org/10.1128/IAI.69.10.5967-5973.2001.
32. **Jaeger T, Budde H, Flohé L, Menge U, Singh M, Trujillo M, Radi R.** 2004. Multiple thioredoxin-mediated routes to detoxify hydroperoxides in *Mycobacterium tuberculosis*. Arch. Biochem. Biophys. **423:**182–191. http://dx.doi.org/10.1016/j.abb.2003.11.021.
33. **Li Y, He Z.** 2012. The mycobacterial LysR-type regulator OxyS responds to oxidative stress and negatively regulates expression of the catalase-peroxidase gene. PLoS One **7**(1):e30186. http://dx.doi.org/10.1371/journal.pone.0030186.
34. **Rojo F.** 2009. Degradation of alkanes by bacteria. Environ. Microbiol. **11:**2477–2490. http://dx.doi.org/10.1111/j.1462-2920.2009.01948.x.
35. **Ron EZ, Rosenberg E.** 2002. Biosurfactants and oil bioremediation. Curr. Opin. Biotechnol. **13:**249–252. http://dx.doi.org/10.1016/S0958-1669(02)00316-6.
36. **Schnappinger D, Ehrt S, Voskuil MI, Liu Y, Mangan JA, Monahan IM, Dolganov G, Efron B, Butcher PD, Nathan C, Schoolnik GK.** 2003. Transcriptional adaptation of *Mycobacterium tuberculosis* within macrophages: insights into the phagosomal environment. J. Exp. Med. **198:**693–704. http://dx.doi.org/10.1084/jem.20030846.
37. **Emtiazi G, Knapp JS.** 1994. The biodegradation of piperazine and struc-

turally-related linear and cyclic amines. Biodegradation **5:**83–92. http://dx.doi.org/10.1007/BF00700633.
38. **Whistance GR, Brown BS, Threlfall DR.** 1970. Biosynthesis of ubiquinone in non-photosynthetic Gram-negative bacteria. Biochem. J. **117:**119–128.
39. **Søballe B, Poole RK.** 2000. Ubiquinone limits oxidative stress in *Escherichia coli*. Microbiology **146:**787–796.
40. **Chattopadhyay MK, Tabor CW, Tabor H.** 2003. Polyamines protect *Escherichia coli* cells from the toxic effect of oxygen. Proc. Natl. Acad. Sci. U. S. A. **100:**2261–2265. http://dx.doi.org/10.1073/pnas.2627990100.
41. **Tkachenko A, Nesterova L, Pshenichnov M.** 2001. The role of the natural polyamine putrescine in defense against oxidative stress in *Escherichia coli*. Arch. Microbiol. **176:**155–157. http://dx.doi.org/10.1007/s002030100301.
42. **Hofmann J, Ashry AENE, Anwar S, Erban A, Kopka J, Grundler F.** 2010. Metabolic profiling reveals local and systemic responses of host plants to nematode parasitism. Plant J. **62:**1058–1071. http://dx.doi.org/10.1111/j.1365-313X.2010.04217.x.
43. **Woluck BA, Communi D.** 2006. *Mycobacterium tuberculosis* possesses a functional enzyme for the synthesis of vitamin C, L-gulono-1,4-lactone dehydrogenase. FEBS J. **273:**4435–4445. http://dx.doi.org/10.1111/j.1742-4658.2006.05443.x.